PULSED, SUPERSONIC FUEL JETS - THEIR CHARACTERISTICS AND POTENTIAL FOR IMPROVED DIESEL ENGINE INJECTION.

Author:
Milton, Brian

Publication details:
Advances in Computational Heat Transfer III
1-5670-174-2 (ISBN)

Event details:
ICHMT International Symposium on Advances in Computational Heat Transfer
Norway

Publication Date:
2004

DOI:
https://doi.org/10.26190/unsworks/687

Proceedings of CHT-04
ICHMT International Symposium on Advances in Computational Heat Transfer

April 19-24, 2004, Norway

CHT-04-K5

PULSED, SUPERSONIC FUEL JETS - THEIR CHARACTERISTICS AND POTENTIAL FOR IMPROVED DIESEL ENGINE INJECTION.

B. E. Milton
School of Mechanical and Manufacturing Engineering,
University of NSW, Sydney, Australia 2052
Correspondence author. Fax +61 2 9663 1222 Email: b.milton@unsw.edu.au

ABSTRACT. High pressure fuel injection has provided considerable benefits for diesel engines, substantially reducing smoke levels while increasing efficiency. Current maximum pressures provide jets that are at less than the sonic velocity of the compressed air in the cylinders at injection. It has been postulated that a further increase into the supersonic range may benefit the combustion process due to increased aerodynamic atomisation and the presence of jet bow shock waves that provide higher temperatures around the fuel. Pulsed, supersonic injection may also be beneficial for scramjet engines. The current program is examining pulsed, supersonic jets from a fundamental viewpoint both experimentally and numerically. Shock wave structures have been viewed for jets ranging from 600 to 2,400 m/s, velocity attenuation and penetration distance measured, different nozzle profiles examined and autoignition experiments carried out. Inside the nozzle sac, numerical simulation using the Autodyne code has been used to support an analytic approach while within the spray, the Fluent code has been applied. Although the modelling is extremely complex, global comparisons show good agreement with experiment. Hence, information on the mixing zone can be inferred. While the benefits of supersonic fuel jets have not yet been defined, it appears that some earlier claims regarding autoignition at atmospheric conditions were optimistic but that increased evaporation and mixing are probable. The higher jet velocities are likely to mean that wall interactions are increased and hence matching such injectors to combustion chamber size and airflow patterns will be important.

INTRODUCTION

Fuel injection and the subsequent spray formation is a key element in the technology of all internal combustion engines, whether these be gas turbines, spark ignition or compression ignition (diesel) engines. The last is the most demanding because:

- a separate injection event of very short duration occurs every second cycle (i.e. at half the engine speed) in a typical four stroke engine.
- the injection must be of very high pressure as it is into the cylinder towards the end of compression. Note that diesel compression ratios are very high.
- the injection timing controls the combustion initiation and hence must be precise.
- the fuel and air mass flow rates are not in a fixed ratio and hence an accurate injection duration related to the injection pressure is necessary to provide the correct fuel quantity at each injection for the particular speed/load operational point.
- the injection process is fundamental to the atomisation, evaporation and mixing of the fuel and hence is a controlling factor in combustion efficiency and emission levels.

Diesel engines play an increasingly significant role in many aspects of modern society dominating the heavy road transport, agriculture, mining and marine sectors and being of considerable importance in rail transport, power generation and pumping. With increasing legislative control over engine emissions and the requirement, often contradictory, for improved fuel efficiency, there have been many changes in recent years. One of the most important developments has been in the area of fuel injection. This is not new as Rudolph Diesel himself undertook extensive research into air blast type atomisers during the original development of his engine in the 1890s [1]. However, for a long period after the introduction of single fluid (fuel only) systems, mechanical injection dominated from the first to the last decade of the 20^{th} century. This included distributor pumps, in-line pumps and unit injectors although, until recently, the last were used only on very large engines. Then, as the need to control particulate matter (PM), of which exhaust smoke is a large component, and nitrogen oxides (NO_x) simultaneously, new types of systems were introduced. These were the mechanical/solenoid controlled electronic unit injectors (EUI), the constant high pressure pump/solenoid controlled common rail types (CRI) and the hydraulically actuated, electronically controlled unit injector (HEUI) with a constant, medium pressure oil pump and an amplifying piston within the injector. They essentially allow both very high pressure injection to provide improved fuel atomisation with control of the fuel timing and delivery from the engine management system. Typical data on the maximum pressures for various systems currently in use are:

- Distributor and in-line pumps, 75 and 110 MPa respectively.
- Mechanical and EUI unit injectors, 100 to 200 MPa
- Common rail injectors, 140 to 180 MPa
- HEUI types 160 to 230 MPa

Hence, the maximum injection pressures (ie, in the nozzle sac) of the different types range from about 75 to 230 MPa in systems currently, or shortly to be, in production. For a small nozzle diameter and intermittent injection such as that in a diesel engine, a coefficient of velocity, C_v is about 0.6 to 0.7 and the corresponding jet velocity immediately at the nozzle exit ranges between 255 and 520 m/s. Typically, the air in a diesel engine during the injection process is at about 750 K with an acoustic velocity of about 550 m/s. Hence, the Mach number of the jet lies is subsonic un the approximately M = 0.45 to 0.95 range.

Further increases in injection pressures will render the jet velocity supersonic with a consequent alteration to the external flow. Leading edge shock waves will eventuate with consequential modification of the shape of the spray and an increase in the local air temperature due to the shock entropy increase. Surface wave phenomena that influence the initial jet breakup will become more significant and the higher velocities will increase the shear-induced atomisation. Overall, further enhancement of the jet atomisation, evaporation and mixing processes and a reduction in the ignition delay period are possible. It has been postulated [2,3,4] that fuel jets of sufficiently high supersonic Mach numbers may autoignite spontaneously in air at atmospheric conditions.

While diesel engines may benefit from such fuel jets in the low supersonic range, even higher Mach number jets may have significance in other applications. One of these is in scramjet (supersonic combustion ram jet) engines that are being considered for sub-orbital flight. These rely on the strong oblique shocks formed at the intake in hypersonic flight to provide sufficiently elevated air conditions for the combustion to take place by direct fuel injection into the very fast flow. For this to be practical, the combustion must be completed within the extremely short residence time within the combustion chamber. This places huge demands on the physical and chemical processes involved in the spray atomisation, fuel evaporation, mixing and ignition. While hydrogen has been used to date, there are significant advantages in conventional liquid fuels but their mixing and evaporation is relatively slow. Intermittent jets have significant advantages over continuous ones in

mixing rates. A subsonic intermittent jet injected into a supersonic air stream [5] is shown on Figure 1. Here, the shock waves induced by the interaction of the supersonic air and subsonic liquid help to deform and break up the jet. A supersonic jet with its own shock pattern would result in even more complex shock wave structures due to the interactions of the two shock forming systems and a further increase in atomisation rates is likely.

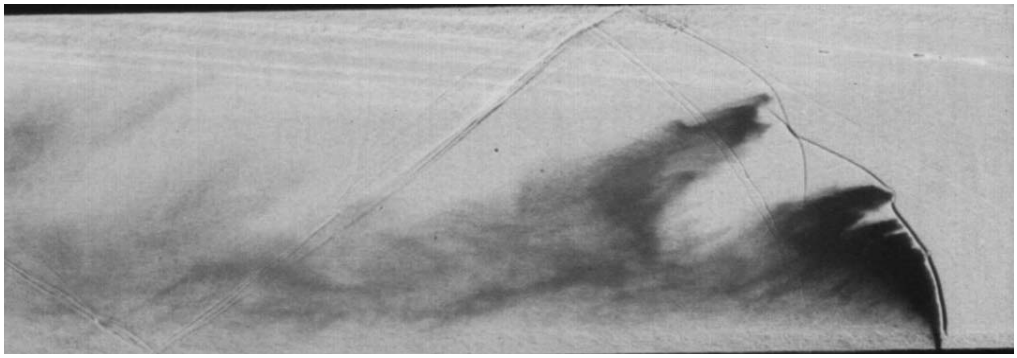

Figure 1. Diesel fuel injected at 70 MPa (~ 300 m/s) into a supersonic air stream at M = 1.9

To date, there has been only limited research on intermittent, supersonic jets, much of this directed towards jet cutting and cleaning processes that require a coherent jet [6,7,8]. Atomisation has not been the prime criteria. This paper deals with current work on very high velocity jets with the aim of establishing a fundamental understanding of the processes involved preparatory to combustion. Much of the work to date has been towards developing an understanding of the driving processes and an experimental evaluation of the jet, shock interactions. Also, there has been considerable computational modelling of the spray, this being important for understanding some of the details that are difficult to measure experimentally and for the development of sub-models for the various engine codes that have been of enormous importance in modern engine development.

DIESEL FUEL JETS.

An intermittent, diesel fuel jet requires a high pressure upstream of the nozzle that is applied rapidly for a short time period. This can be obtained by use of either a piston type plunger accelerated into a fluid filled cylinder or a rapidly opened valve from a more or less constant, high pressure accumulator (common rail). The former is typical of the mechanical systems in which the plunger is driven by a cam while the latter is representative of the newer common rail types. The HEUI types are similar to the common rail types in the supply of the fluid to the driving side of their stepped internal piston but somewhat like the mechanical systems on its injection side. All injectors have a needle that closes off the nozzle holes at lower pressures to ensure that no unwanted flow occurs. The needle is lifted by hydraulic pressure as the injection pressure is applied. This opening (and closing) pressure is well below the maximum pressure achieved during injection.

Regardless of the system used to obtain the high pressures, the nozzle sac (and any connecting lines to and from the high pressure source) must undergo a wave motion that is re-reflected backwards and forwards upstream of the nozzles several times during injection. This will build up the pressure at the nozzle entrance in a series of discrete jumps. For low injection pressures, less than about 100 MPa, this is not particularly significant but it becomes quite pronounced as the injection pressure is raised. The fuel line distortion due to this pulsation is a major reason why pressures are limited in systems with fuel pumps remote from injectors.

The formation of the jet outside the nozzle is therefore subject to this intermittent pressure rise. It is also a function of the design of the nozzle interior. For a simple, smooth nozzle, for example, with a rounded entry or a conical shape, the flow from the sac to the spray is fairly smooth. Real diesel injectors, however, have convoluted internal passageways and sharp edge entries to the parallel nozzles that cause turbulence, separation and cavitation in the flow (see Figure 2). It has been shown in recent research [9,10,11] that this is of considerable significance in atomising the spray.

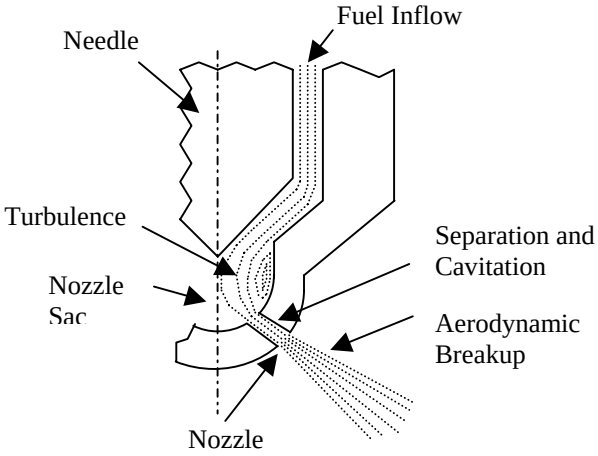

Figure 2. Flow in a multi-hole diesel nozzle showing possible jet breakup mechanisms

Until recently, the spray exiting the nozzle was described as a coherent liquid core for the initial period of its development, narrowing during atomisation. The core end-location called the “breakup length” was often inferred as being up to 100 times the nozzle diameter. It was assumed that this core gradually decreased in diameter with ligaments, sheets, clumps and droplets being sheared off aerodynamically. Recent papers have indicated that the breakup length is actually very short, perhaps a few diameters at the most and an atomised spray exists very soon after the nozzle exit. One approach has been to obtain empirical formulae for the breakup length and many such relationships exist. Some of the best known are those of Reitz et al. [12] and Hiroyasu et al. [13].

After breakup, the spray diverges as a cone of atomised droplets. In the early part of this main spray formation, the physics is somewhat obscure as there may be ligaments, clumps and droplets that continually separate and undergo secondary atomisation, collision and merger. Overall, the separation dominates as the diameter grows and the spray reaches a more dispersed state where individual packages of fluid or droplets can be tracked. Droplets are not uniform across the jet, being smaller towards the outer edge. The surface area of the liquid now grows rapidly and it is here that the evaporation and mixing rates become high. Air is entrained into the spray. As the fuel vapour diffuses outwards from the drops and the air inwards towards them, the mixture will eventually fall locally within the flammability range. As long as the temperature and pressure are suitable, as happens due to the high compression ratio in a diesel engine, ignition will then occur.

MODELLING OF DIESEL SPRAYS.

Modelling of fuel sprays is an important component of internal combustion engine simulation as the spray has an important effect on the mixture preparation within the cylinder, particularly in the new gasoline direct injection (GDI) engines and diesel engines which are highly stratified. To understand the spray processes, spray modelling needs to be carried out. Further, for 3D, fluid mechanical engine models, a known size, velocity, location and trajectory of the fuel droplets is essential so that the combustion can be located within the appropriate computational cells.

Early empirical models were relatively simple. The flow exiting the nozzle was calculated from the known time dependent, injection sac (or line) pressure trace. A quasi-steady modelling using the geometrical nozzle area and a coefficient of discharge then allowed the average velocity leaving the nozzle to be determined. Empirical formulas exist for the spray angle, droplet size (Sauter Mean diameter, SMD) which reduces as the droplets evaporate and the related time dependent droplet penetration and velocity [13, 14]. The droplet velocity distribution at each angle up to the outer cone is also evaluated from experiment. Air entrainment and diffusion models calculated mixture formation continued until combustion conditions were reached. Models such as this were used in a number of codes, for example, that in the diesel and dual-fuel combustion simulations used at UNSW over a number of years. [15, 16, 17].

Model development has progressed to a more theoretically based approach. This includes aerodynamic breakup from the generation of Kelvin-Helmholtz instabilities on the jet surface from which droplets emanate and turbulence and cavitation within the nozzle. A modern injection simulation is described by in [18]. Here, a one-dimensional, time dependent calculation is used to describe the flow from the fuel pump, through the injection lines to the injector. A CFD model is used to simulate the flow past the needle within the nozzle sac, then into the parallel nozzle. Different droplet atomisation models were compared to experiment velocity and SMD measurements, the cavitation model giving the best results although contributions from all modes are likely. There is still much work required on modelling subsonic jets and sprays.

.

SUPERSONIC AND SUBSONIC LIQUID JETS

In any intermittent jet, air is set in motion by the jet head as it emerges from the nozzle and grows in length and diameter. That is, there is a pressure increase ahead of the jet that results in a wave motion being transmitted through the air ahead of it. The highest pressure will exist at the stagnation point at the jet head. The forward air motion from the wave at the side of the jet will be increased by the shear layer and mass transfer from the liquid in the mixing region.

When a subsonic jet injected into quiescent air is compared with a low range supersonic jet (at about 600 m/s, M = 1.8 at ambient conditions), both exhibit a bulbous jet head. In the former, the pressure wave ahead of the jet is not of great significance. Once the jet exceeds sonic velocity, this is no longer the case. Shock waves around the jet become a noticeable feature of the flow. Some of the questions that could be posed are whether the features of the flow (e.g. the breakup length, atomisation and penetration distance) follow a similar pattern to subsonic allowing the same empirical equations to be used and whether the shock wave structures of supersonic jets can modify the fuel ignition qualities.

EXPERIMENTS ON SUPERSONIC JETS.

Background literature. Supersonic liquid jets have primarily been studied as water rather than fuel jets, the prime purpose being cutting or cleaning. As such, most are continuous rather than intermittent jets. Intermittent jets may exceed continuous jet velocities but are harder to generate. In 1958, Bowden and Brunton [7] presented a new technique for this purpose. A high-speed projectile was fired into the rear surface of a liquid in a nozzle sac to accelerate it through a nozzle at the sac front to a high velocity, 1050 m/s being reached in their experiments. This technique is now termed the “Bowden-Brunton” method. In 1967 O’Keefe, et al. [19] using the impact of a 1.77 km/s projectile, measured a water jet velocity of 4.58 km/s. In 1973 Ryhming [20], described the process using a one-dimensional, incompressible flow analysis. For the analysis of a water cannon, Glenn [21] in 1975, extended Ryhming’s work by including the effect of liquid compressibility. As O’Keefe’s study, the liquid shock wave reflection processes within the nozzle was not considered.

In their 1977 work, Field and Lesser [2], experimenting with oil jets, suggested that a spontaneous combustion of the oil might have occurred at high supersonic speeds. In the light of this, Shi [3] and Shi and Takayama [4], who were basically examining water jets, included a study of supersonic diesel jets in their experiments. They used a powder gun arrangement similar to the original Bowden-Brunton technique but reported much greater water jet velocities of 4 km/s. For diesel fuel jets of more than 2 km/s, they found that smoke covered the test chamber at the completion of a run and postulated that it may have been due to combustion. Holographic interferometry was used to visualize the jets and, while not totally clear, there was some suggestion that additional illumination occurred from the jet.

In 1995, Lesser [22] presented the basic mechanics of supersonic jet generation by using a theory called guided acoustic waves. While it was realised that during the supersonic liquid jet generation process either a single, strong shock wave or a multiple shock wave reflections must be involved inside the nozzle cavity, this was ignored in the analysis. In the present work, these effects have recently been included in the analysis and are described in [23].

Apparatus for creating the intermittent supersonic liquid jets. The pressure required to produce a jet is theoretically proportional to the square of the jet velocity but in actuality to a higher index due to increasing losses. Thus, supersonic jets require very high driving pressures, extreme in the high supersonic range. In the low supersonic range, pressures can be obtained by use of the conventional diesel injection systems but high Mach number jets require a different approach. For such jets, rapid pulsing for hours on end as required in an engine presents technical difficulties. However, in the research presented here, the object is to study the fundamentals of supersonic jets and hence a single pulse, short duration jet has been used in the experiments. The same method has been adhered to for consistency throughout the work to encompass low to high supersonic Mach numbers. It is the Bowden-Brunton projectile impact onto the fluid in the nozzle sac.

Collaborative experiments in the program have been carried out at the University of New South Wales, Australia (UNSW) and at the International Shock Wave Research Center, Tohoku University, Japan (ISWRC). The former drove the impacting projectile using a vertical, downward firing, single stage powder gun while the latter used a larger diameter, two-stage light gas gun. The powder gun, Figure 3, described previously [24] achieves velocities of up to 1100 m/s for the 8.0 mm diameter, 10 mm long, 0.65 g cylindrical polycarbonate (PC) projectile. The projectile travels downwards through the pressure relief section, which is designed to diminish the blast wave in front of the projectile and to guide it onto the liquid. The nozzle sac is directly connected to it, being seated in the top wall of the test chamber. Mild steel sac/nozzles were used, in a few cases being case hardened. The nozzle exit diameters, d were varied for different experiments from 0.5 mm to 6 mm diameter. As reported in [27], most experiments were carried out with 0.5, 0.7 and 1mm diameter nozzles with L/d of 2 to 6. The ISWRC apparatus is similar in concept but different in detail, the vertical two-stage light gas gun firing a larger PC projectile of 15 mm diameter, 20 mm length and weight 4.45 g. A projectile impact velocity of 700 m/s was used, this beings the maximum initially available.

In both cases, the liquid was retained in the nozzle using a thin plastic diaphragm seal at the top and bottom of the nozzle. Its low strength relative to the impact force of the projectile means that the opening pressure for the nozzle (equivalent to needle lift) is very low. Projectile and liquid jet velocities were measured in both systems using a laser beam interruption method, two closely spaced laser beams being placed as close as possible to the nozzle exit. In the ISWRC apparatus, for jet penetration and velocity attenuation measurement, six laser beams and a high-speed camera apparatus were employed in separate experiments.

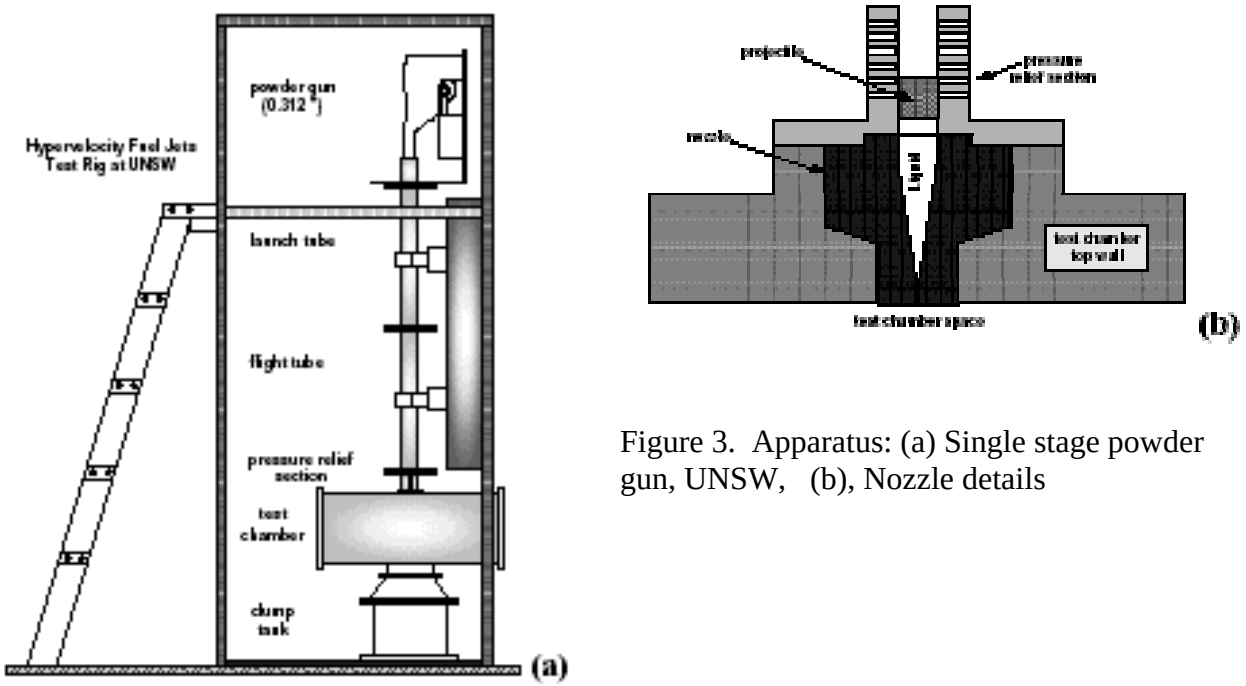

Figure 3. Apparatus: (a) Single stage powder gun, UNSW, (b), Nozzle details

Nozzle sacs were designed to accommodate the projectile impact. A cylindrical sac with a tapered conical contraction to the cylindrical nozzle was used. While a range of cones were tested, the most common had a 20 ^{o} included angle (UNSW) and 47 ^{o} (ISWRC). In the UNSW apparatus, exponential and hyperbolic nozzle convergence profiles were also tested. Additionally, the ISWRC experiments carried out experiments on a stepped (i.e. no conical convergence) orifice to stimulate turbulence and cavitation.

Jet and shock wave shapes from experiment. Shock wave shapes from the conical nozzles at UNSW are shown on Figures 4 and 5 for a low (600 m/s, M=1.8) and a high Mach number (1800 m/s, M=5.3) jet respectively, both into atmospheric air. At the low jet velocity, the jet emerged with a flat front that changed rapidly with jet growth to the bulbous profile similar to that found in subsonic jets. A detached shock wave was clearly visible ahead of the jet from the time of its formation. At higher Mach numbers, the shock wave became attached to the jet head forming an oblique system similar to solid body interactions. This distorted the jet head, making it sharper as the jet velocity rose as can be seen on Figure 5. Some random irregularities, evident in the photographs, occurred in the jet head that may have been due to turbulence generated within the nozzle sac or to distortion of the nozzle itself caused by the high pressure. However, as will be discussed later, the pressure maximised after the initial jet was formed and so nozzle distortion is more likely to affect the later portions of the jet rather than the jet tip. Hence, the fluid mechanics inside the nozzle is the most likely cause. Also of note was that, at the higher Mach numbers, a secondary shock wave existed alongside the jet, as indicated by the arrows in the centre photograph.

Only high Mach number jets (1800 m/s, M= 5.3) were examined at ISWRC, these being depicted on Figure 6. Comparing these profiles with those of Figure 7(a) for hardened nozzles suggests that the scaling of the experiment has only a small effect. The difference between Figure 5 and 6 profiles is probably due to the stainless steel nozzles used at ISWRC. In the ISWRC experiments, the secondary shock wave system is clearer and a tertiary system is also present. The latter are also visible in some of the UNSW experiments. Even at high Mach numbers with an attached bow shock, the head still tended to form a bulbous shape, narrowing behind to the long core. It then thickened again at the secondary shock positions. In all cases, near the nozzle exit, a spray zone

existed with a higher conical included angle than the flow ahead of it. Note that it is possible that hydraulic flip has occurred in some cases and this needs further investigation.

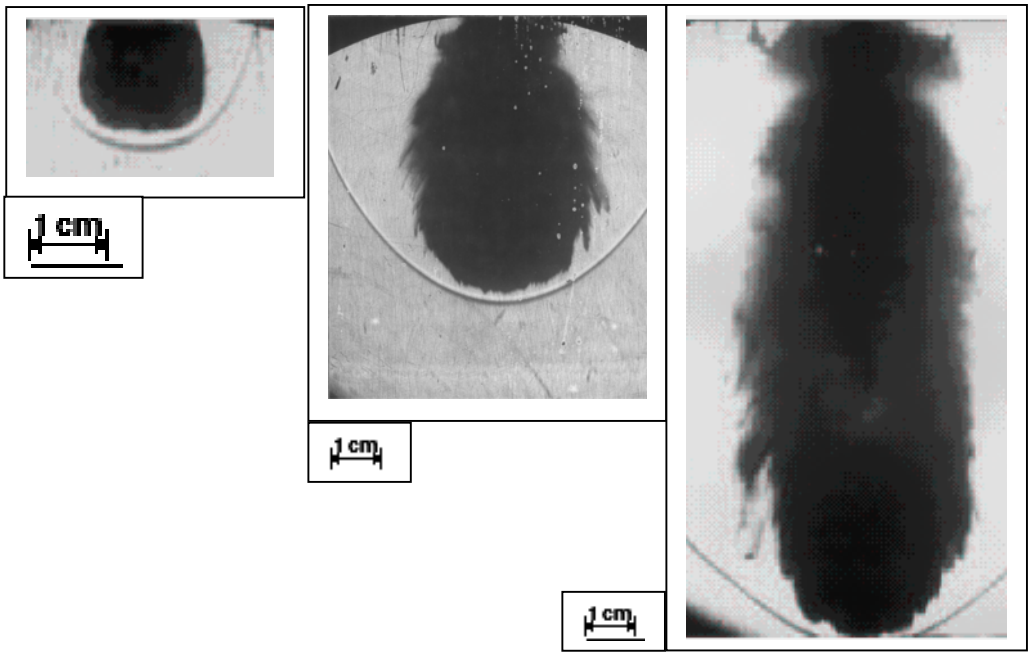

Figure 4. Water jet from a conical 5 mm. nozzle at M = 1.8 (600 m/s) showing the jet development and detached bow shock wave (UNSW experiments).

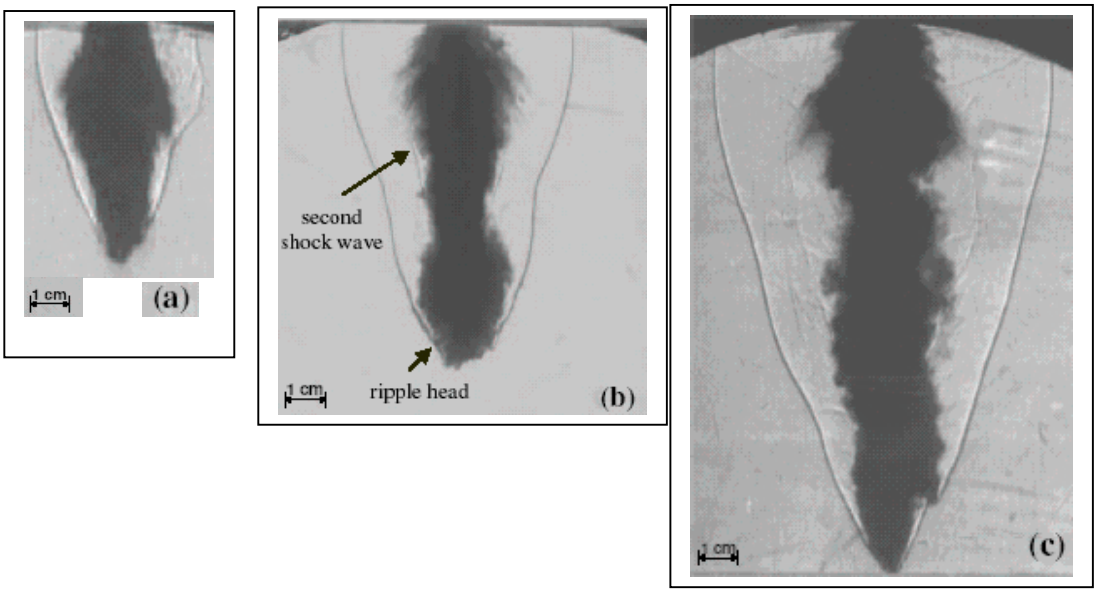

Figure 5. Diesel fuel jet from a 1 mm. nozzle at M = 5.3 (1800 m/s) showing the jet development. (UNSW experiments).

The effect of nozzle differences is illustrated on Figure 7. This shows jets from a hardened conical nozzle, a mild steel hyperbolic nozzle and a stepped nozzle. The hardened nozzle exaggerated the patterns discussed above with the long, narrow core clearly visible. The hyperbolic (and exponential) nozzles showed a smoother, more uniform jet shape indicating that random effects from the flow into the sharper, conical entry carry over into the spray. The jet head from the stepped

nozzle was the most irregular and bulbous. Even at the highest initial velocities of around 1560 m/s, the flatter head reduces the conical shock to a more rounded shape. At 126 μs, it is attached whereas at 226 μs, it has separated and thereafter moves progressively ahead of the jet. This is likely to be due to both the broader spray head and the more rapid attenuation after the first 100 to 200 μs.

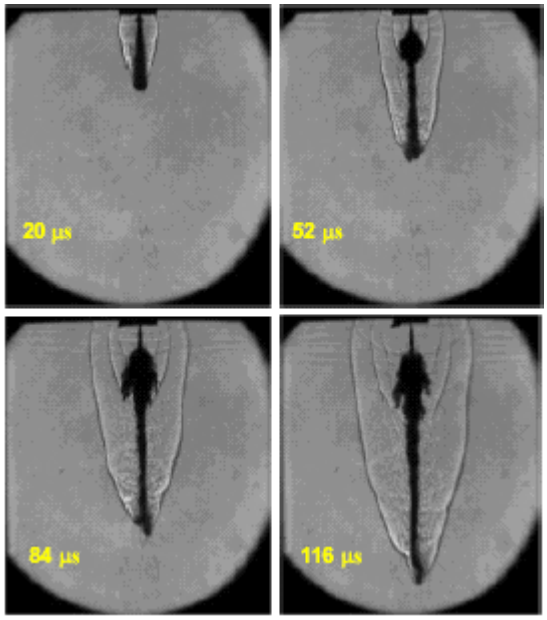

Figure 6. Diesel fuel jet at M = 5.3 (1800 m/s) showing the jet development. (ISWRC experiments).

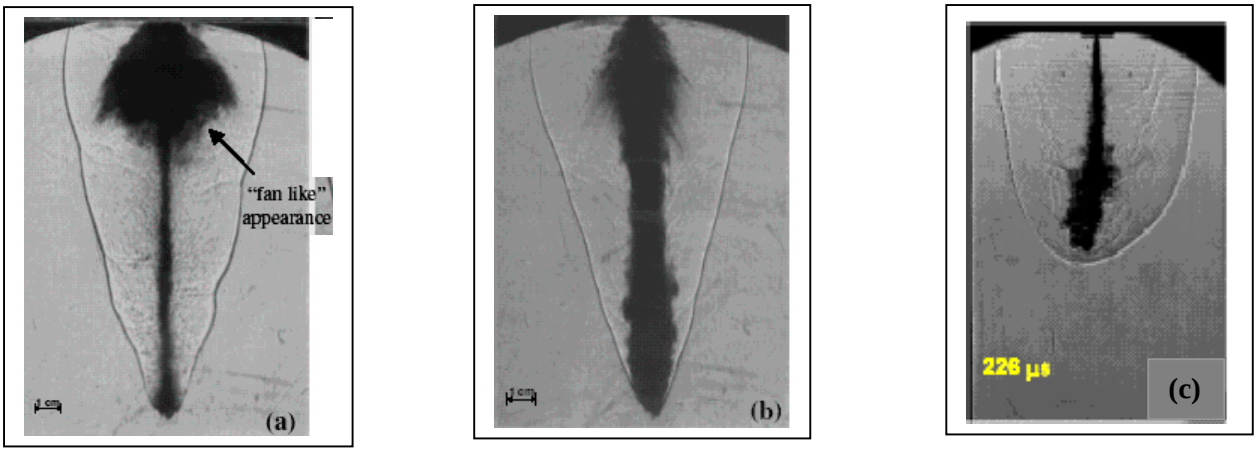

Figure 7. Diesel fuel jets from (a) hardened, conical nozzle, 2350 m/s (b) hyperbolic nozzle, 1850 m/s (c) stepped nozzle, 1560 m/s showing the jet development. Experiments (a) and (b) are UNSW, (c) is ISWRC. All nozzles 1 mm diameter

Jet velocities. One of the immediate aims of the experiments was to obtain the maximum jet velocity. As noted above, jet velocities of up to 4000 m/s had been reported from similar techniques. The present experiments both at UNSW and ISWRC were unable to achieve such values. At the maximum current capability, as the nozzle size was decreased, the jet velocity rose. However, the maximum that could be obtained in these experiments were as on Table 1:

Table 1
Maximum measured jet velocities

Nozzle profile	Nozzle area ratio	Nozzle material	Tests at:	Max.velocity, m/s
Conical	256:1 (0.5 mm)	Mild steel	UNSW	1850
Conical	130:1 (0.7 mm)	Mild steel	UNSW	2000
Conical	64:1 (1 mm)	Mild steel	UNSW	1800
Conical	130:1 (0.7 mm)	Hardened	UNSW	2500
Conical	225:1 (1 mm)	Stainless steel	ISWRC	1800
Hyperbolic	64:1 (1 mm)	Mild steel	UNSW	1900
Exponential	64:1 (1 mm)	Mild steel	UNSW	1850
Stepped	225:1 (1 mm)	Stainless steel	ISWRC	1560

A nozzle of area ratio 130:1 gave the best results. A smother nozzle shape provided small increases while a stepped nozzle reduced the velocity. The nozzle material was of greater significance, the hardened nozzle showing significant improvement. However, these nozzles cracked during the run and were not reusable. The normal, mild steel nozzles exhibited some distortion but were not destroyed in a single test. Measurements indicated that reuse was possible although in the interest of accuracy, this was not done. For the low Mach number (M = 1.8) tests, nozzles showed no permanent distortion or erosion. Hence, they could be used for many runs.

Jet Attenuation and Penetration. Using the series of six lasers (and a high speed camera, results not shown here) in separate tests at ISWRC, the profile of jet penetration with time was determined. Differentiating this gives the jet velocity/time relationship from which the attenuation profile was plotted as on Figure 8(a).

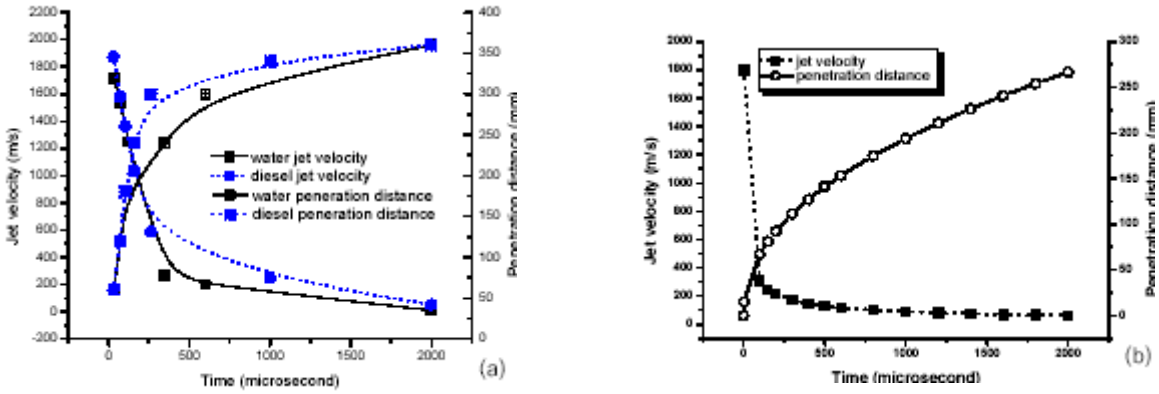

Figure 8. Measured time dependent jet velocities and jet penetration:
(a) conical nozzle, (b) calculations from the conventional subsonic formulae of [14].

The initial velocity of the diesel fuel jet was slightly higher than that of water, the exact values being 1863 m/s and 1714 m/s respectively. The diesel velocity attenuation was slightly lower, particularly after the first 300 μs although by 2000 μs there is little difference. Hence the diesel penetrates further for most of the injection period. The reduction in velocity is quite high during the first 300 μs. A comparison, [25], of these test results with the estimation of jet velocity attenuation and penetration distance obtained from the use of a conventional, empirical diesel fuel spray formula [14] is shown on Figure 8(b), calculated for an initial diesel velocity of 1800 m/s. The trends are similar although the experiments indicate higher values of both velocity attenuation and penetration by 20 to 30%. This indicates that the subsonic formula, while needing some

improvement, provides a reasonable starting point for estimates. Some penetration estimates at 1 ms (a typical ignition delay time in a diesel engine) for 600, 1200 and 1800 m/s jets are about 117, 161 and 194 mm respectively. These are moderately large distances and may place a limitation on the use of extreme pressure injection in smaller engines depending upon whether the shock waves can further shorten the ignition delay. Note that the stepped nozzle has a lower initial velocity and higher attenuation and therefore does not penetrate so far.

Autoignition of the fuel. An extensive experimental examination was carried out in the UNSW facility to determine if autoignition occurred. Tests covered a wide range of conditions, jet velocity ranging from 1800 to 2000 m/s, test chamber air heated from ambient to 100^{o}C and fuels from conventional diesel with a cetane number, CN of 45 to pure cetane (CN = 100). Note that, as cetane number increases, so does the ease with which the fuel auto-ignites. Measurement techniques looked for visible light from a combustion source by exposure to photographic plate with the test chamber darkened and sampling of the post combustion gases for traces of carbon dioxide (CO_2), carbon monoxide, (CO) and nitrogen oxides, (NO_x). Overall, it was assessed that, for these jets, no autoignition resulted. There was ample evidence of post-test smoke in the test chamber but this was due to fuel vaporisation. This does not yet indicate that low temperature autoignition is not possible. A different nozzle geometry or higher jet velocities may contribute. However, the additional evaporation does indicate that the fuel may be better prepared for ignition than with a conventional spray. Currently, tests are underway to examine the enhancement of low cetane number fuels (i.e. fuels not suitable for direct use in diesel engines) such as butane, propane, ethane and eventually methane to see if supersonic jets can improve their ignition characteristics.

NUMERICAL ASSESSMENT OF DRIVING SUPERSONIC JETS

One-dimensional theory. A general method of predicting the driving pressure from the projectile impact and relating it to the jet velocity is a valuable tool and can help explain such phenomena as. multiple shock wave formation. To do this, a one-dimensional model of the shock wave pressure generation within the cavity has been developed [23]. It requires initial input conditions of projectile mass and velocity at the time of impact, and the liquid mass. The nozzle area was assumed to consist of a single step from that of the sac. On impact, a shock wave moving in the projectile direction is generated in the liquid while another in the projectile is transmitted in the opposite direction. By equating the momentum transfers and the interface velocity, equations can be developed which give the pressure, P, behind the liquid shock and hence the related shock velocity. Normal reflection of this shock from the end-wall of the cavity determines the first pressure pulse that drives the nozzle flow. A series of reflections between the end wall and projectile face incrementally increase the driving pressure at the nozzle entrance. At each reflection cycle, the projectile velocity is assumed to be that of the previous interface. That is, the projectile, liquid interface remains coherent throughout. Each pulse slows the projectile incrementally.

As the projectile and liquid have the same cross-sectional area, the length ratio of the liquid in the nozzle sac to that of the projectile is important. Depending on this value, different wave combinations are possible. This is because there is a maximum quantity of liquid that can be accelerated to conditions compatible to the liquid shock by the original momentum decrement of the projectile. For example, if the liquid slug is very long, the projectile must slow further after it has transferred the appropriate momentum quantity to below the particle velocity behind the shock. If it is very short, the reflected shock from the end of the nozzle sac will re-reflect from the projectile interface while it still transferring the original momentum quanta. In between, a situation will exist where the returning (reflected) shock in the liquid just reaches the projectile as the last of that momentum increment is being transferred. This is referred to here as the “balanced” length, depicted on Figure 9, and used in these calculations. Other combinations will give slightly different answers but require a more complex formulation. A proportion, *F*, of the total momentum

decrement is transferred to the liquid during the forward motion of the shock, the remainder during its return to the projectile. The ratio of the time period, t_f, for the forward motion of the shock in the liquid to that for the shock in the solid to traverse its length, t_c determines F.

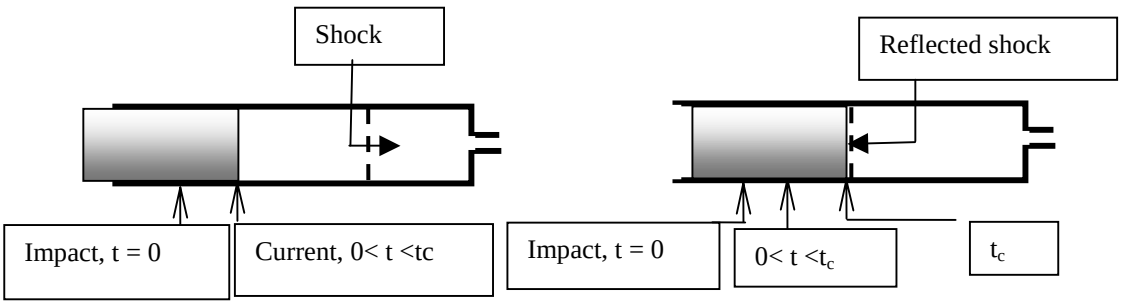

Figure 9. Balanced case for shock motion in the nozzle sac

Assumptions are that normal impact and one-dimensional particle and shock motion occur, that the interface between projectile and liquid in the nozzle is coherent, the nozzle has a single step from sac to exit, and the walls are rigid. The shock wave velocity in both the projectile and liquid, particle velocity, and impact pressure rise P can then be estimated.

$$P = F\,\rho_s C_s \left(V_s - U_{p2}\right) = \rho_1 C_2 U_{p2} \qquad (1)$$

Here, ρ is the density, C the shock velocity. Subscripts (s) relate to the projectile, (1) and (2) to the liquid before and after impact while V_s is the initial projectile velocity and U_p the water particle velocity. By applying the shock Hugoniot relation, the shock wave velocity in both substances can be obtained as in equation (2).

$$\textit{projectile} \qquad C_s = a_s + k_s\left(V_s - U_{p2}\right) \quad \textit{water} \qquad C_2 = a_2 + k U_{p2} \qquad (2)$$

Here a is the sound velocity in the substance and k is a material constant. A solution for U_{p2}, can then be found from which P follows. On reflection of an incident shock wave, a normal reflected shock wave of velocity C_3 returns to the projectile. Determination of the driving pressure and particle velocity just upstream of the nozzle exit follows. The jet velocity, V_j is then obtained by integrating the one-dimensional Euler momentum equation using the Tait equation of state relationship. Subscripts z and a designate the nozzle and atmospheric conditions respectively while A_w and n are constants for water (values are 363.2e+6 and 6.11).

$$V_j^{\,2} = V_z^{\,2} + \frac{2n}{n-1}\frac{\left(P_a + A_w\right)^{\frac{1}{n}}}{\rho_a}\left\{\left(P_z + A_w\right)^{\frac{n-1}{n}} - \left(P_a + A_w\right)^{\frac{n-1}{n}}\right\} \qquad (3)$$

Basically, the numerical work required is simple, involving the simultaneous solution of twelve algebraic equations. These relationships describe the complete cycle from the onset of the impact until the shock wave reflected from the end-wall reaches the projectile. Reflection cycles are repeated until the projectile stops. The $x-t$ diagram of Figure 10 describes the shock reflection in the nozzle sac. A comparison of measured and calculated jet velocities assuming a coefficient of velocity, C_v of 1 for the latter is shown on Figure 11. A typical value of C_v of 0.63 to 0.72 is obtained. This is very reasonable for a pulsed nozzle.

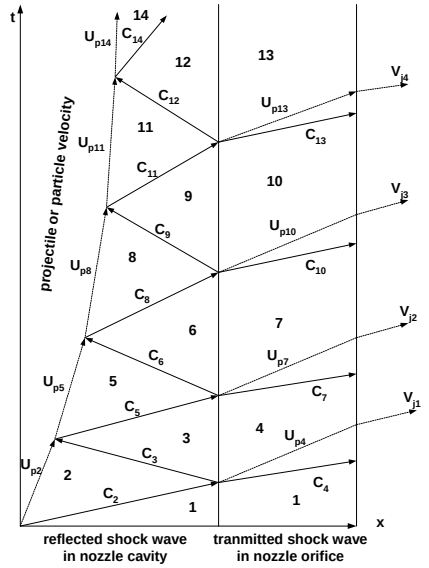

Projectile velocity 1100 m/s,

Figure 10 Typical x-t diagram

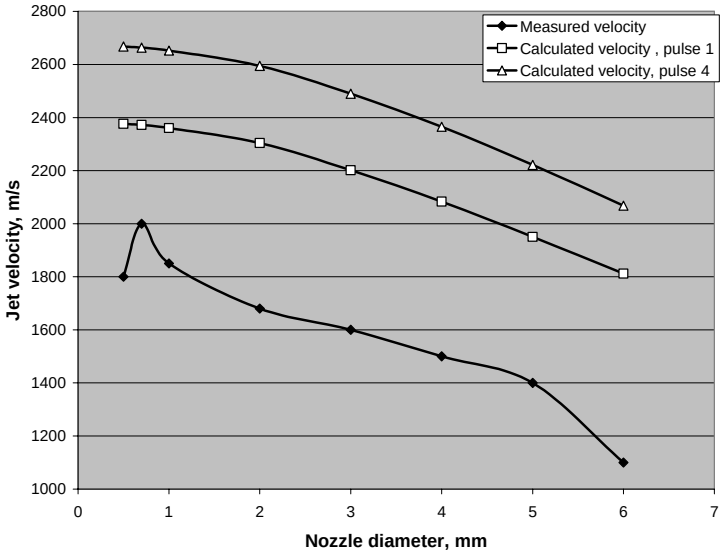

Figure 11 Measured and calculated jet velocity

Estimation of jet velocity for different conditions. Using a similar calculation procedure, projectile characteristics can now be considered. Nozzle velocity coefficients are assumed to remain unaltered while the calculations are for a 1 mm orifice (area ratio 64:1).

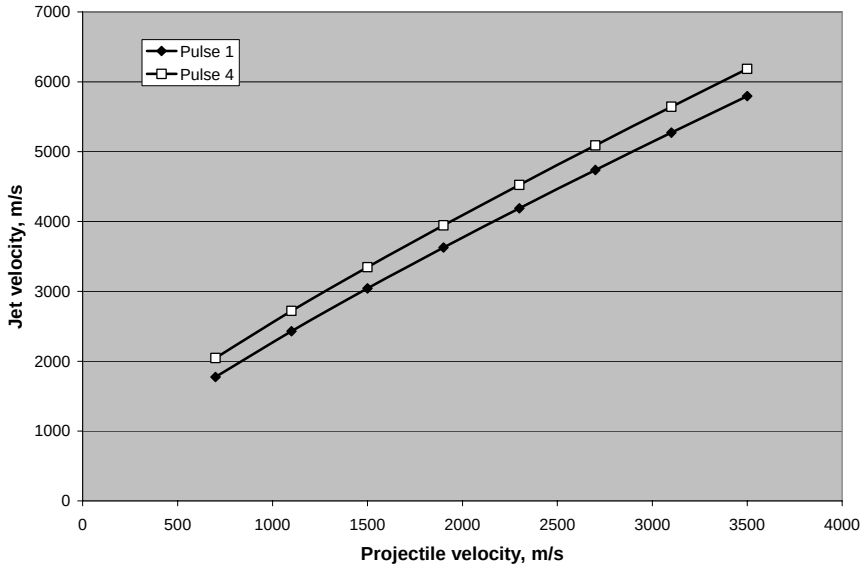

Figure 12 Relationship between projectile and jet velocities

Interestingly, the projectile size does not alter the result as long as it remains of the same material. Hence, the basic parameter affecting the jet velocity is the projectile impact velocity. This is shown on Figure 12. To obtain a jet velocity of 3000 m/s on the fourth pulse, assuming a realistic C_v = 0.63, requires an impact velocity of 2500 m/s. For a 4000 m/s jet, the projectile would have to reach a velocity of at least 3800 m/s. This is extremely high.

The nozzle sac pressures at these velocities become immense. These are shown on Figure 13. For a 3000 m/s jet, the values reached would be 16.5 GPa (pulse 4) while for 4000 m/s it would be about 34 GPa. The latter is impossibly high. The effects on the liquid at these pressures are unknown but it is unlikely that the Tait equation would still represent its properties while the effect on the projectile is difficult to estimate. Even at the lesser 3000 m/s jet velocity, it is likely that the nozzle would distort or shatter well before the peak jet velocity was reached. Also, the pressure wave system within the walls of the nozzle would become significant. These effects would further reduce the coefficient of velocity and the potential of the system to generate high jet velocities.

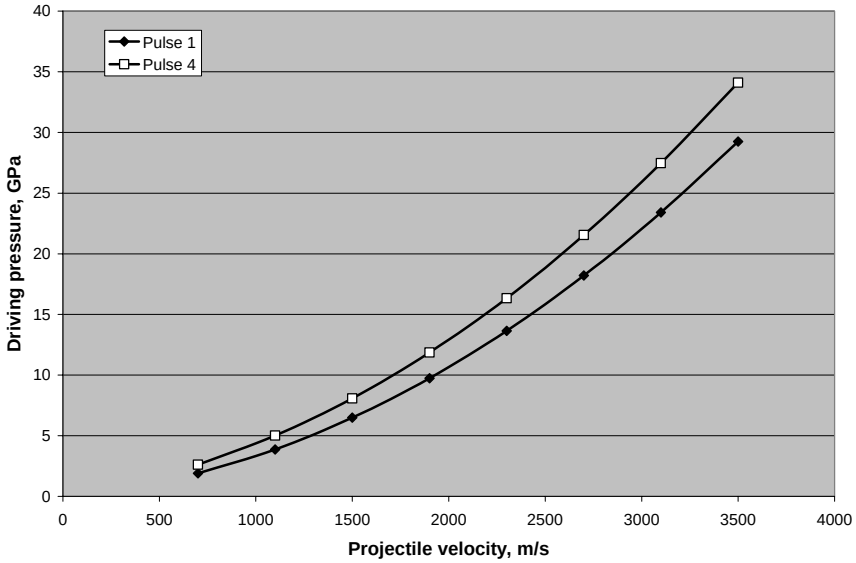

Figure 13 Estimated nozzle sac pressure to obtain jet velocity

Computations from the Autodyne code The two-dimensional interactive non-linear dynamic analysis software (AUTODYN-2D TM , Century Dynamics Inc.) was used at ISWRC to simulate this driving event. This numerical code can treat the Lagrangian and Eulerian frames in a fully coupled way providing a great flexibility in simulating complex wave and material interactions among different phases. The dimensions and the projectile speed used in the simulation of 1100 m/s matched the UNSW facility. The hydrodynamic behavior of the different materials in different co-ordinate systems is solved in a fully coupled way using the code. The numerical code has a data library and detailed mechanical properties of most typical materials such as those used in the current study are down loaded automatically during the calculations.

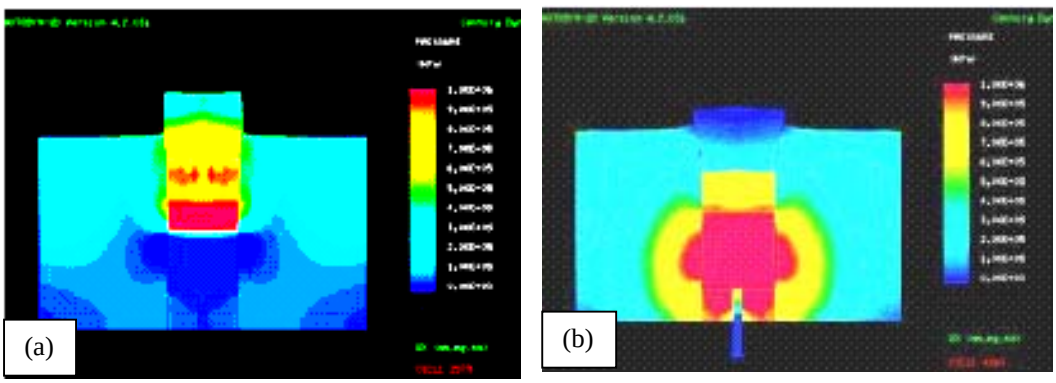

Figure 14. Typical pressure contours from the Autodyne calculations. (a) At 4.5 μs (b) At 13.5 μs

Figure 14 shows the pressure distributions at 4.5 and 13.5 after the impact. In Figure 14(a), a shock wave is immediately generated upon the projectile impact that propagates in the water and through the stainless steel nozzle body. The pressure and flow (particle) velocity behind the shock wave in water are around 1GPa and 500 m/s respectively. These conditions are close to the 1D analysis predictions. Figure 14(b) shows the results after the liquid shock wave is reflected at the nozzle. Further calculations through re-reflection are available. When the water jet is well developed, it reaches a maximum speed of 1420 m/s. Note that this is less than measured in the experiments while the 1D analysis is, more realistically, greater. The use of the code is beneficial although further exploration is necessary.

CFD EXAMINATION OF THE SUPERSONIC LIQUID SPRAY

Previously, in the simulation programs used for diesel and dual fuel combustion at UNSW, empirical or quasi-empirical models of the diesel injection were used. For the present research, it was felt that these were not suitable for the following reasons. Firstly, the shape of the conical bow shock wave around the jet was needed to compare with shadowgraph experiments, the conditions generated by it being important for a further understanding of the fuel/air mixing preparatory to combustion. Secondly, the shape of the jet itself was critical in validating the CFD approach from the experimental results. Finally, as many factors related to intermittent, supersonic jets such as the breakup and atomisation processes were unknown, validation would best be obtained by comparisons with steady, supersonic jet cases. A conventional CFD approach could more easily work through such a sequence. Hence, the proprietary CFD code, FLUENT was chosen. Experimental studies are unable to capture intricacies within the jet core close to the nozzle and are intrusive leaving details of the internal structure of the jet open to question. The use of CFD has been advantageous in starting to evaluate these. However, even CFD presents many difficulties.

In modelling such a complex process as a transient, supersonic deformable surface, several factors need consideration. In particular, these are the shock wave formation ahead of the jet and the density variations from the surrounding air, through the mixing layer to the liquid core. While several turbulence approaches were examined, the k-ε model was found to be the only suitable solution due to convergence problems with the others.

The approach followed has been:

- To use a computational domain from the nozzle exit for a wide field around the jet
- To assume that the inflow conditions are steady for the lifetime of the jet.
- To develop the solution procedure in order against
  i. Steady, supersonic flow of air over solid bodies of jet-like shapes
  ii. Steady, supersonic flow of air over water vapour jets.
  iii. Steady, supersonic flow of air over liquid jets
  iv. The flow of unsteady, supersonic vapour jets into air.
  v. The flow of unsteady, supersonic liquid jets into air.

The last, of course, is the case studied experimentally. The CFD studies to date have been predominantly confined to the lower end of the experimental supersonic velocity range, i.e. 600 m/s although some runs at 2000 m/s were carried out for case i. above. The computational times for the higher velocities are extremely long and not practical at this stage.

The CFD to date has considered only water as the liquid. This is because its properties are widely available and, being a single component substance only, non-variable. Diesel fuel contains many components, at least 16 being required to define it properly. Experiments were carried out on water as well as on diesel jets and the former are used for comparison with the CFD. While some differences between the two fluids are evident in the experiments, these are generally small.

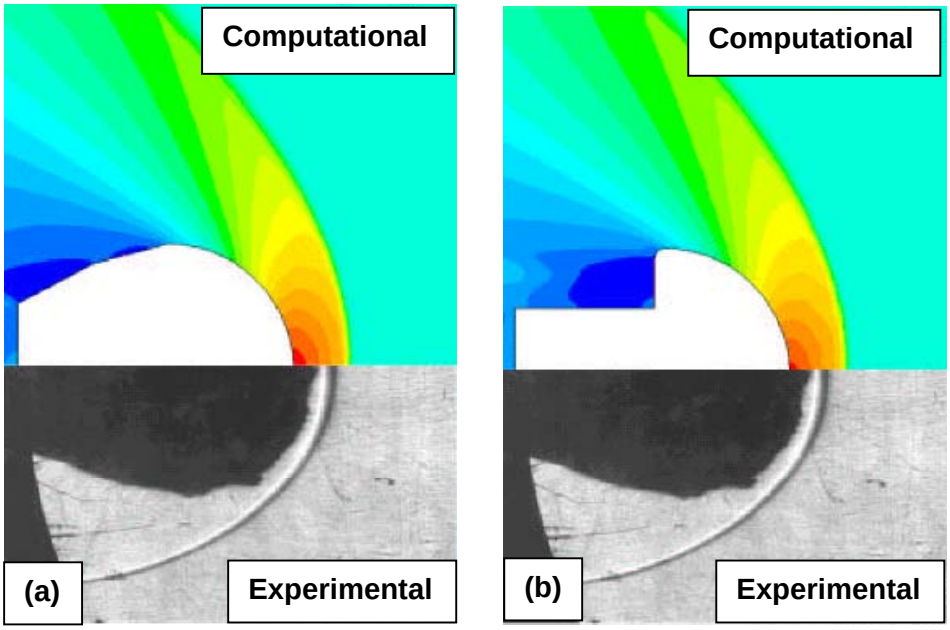

Figure 15. Bow shocks on solid body shapes, V = 600 m/s. (a) Tapered profile (b) Cavity profile

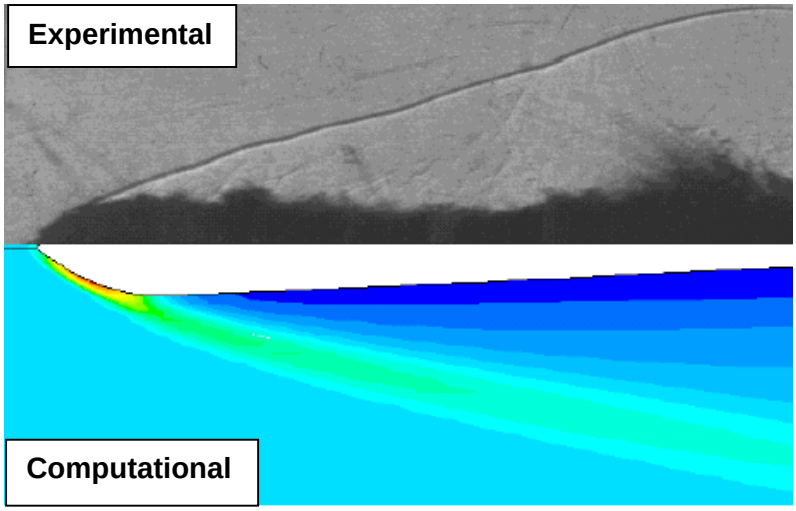

Figure 16 Bow shocks on a jet-like solid body shape, V = 2000 m/s

Solid body assessment of the air shock wave system. The first consideration is whether the shock wave system can be predicted with reasonable accuracy by the CFD code. An initial calibration against a sphere where ample experimental data is available provided good agreement in the bow shock wave shape and stand-off distance [26]. For the jet with a velocity of 600 m/s (Mach number 1.8 in air at ambient conditions), the jet geometry was chosen as solid bodies with profiles, as shown on Figure 15, estimated from the corresponding experiments. The shock wave shapes from simulation and experiment are also illustrated on Figure 15. The comparison shows that the shock stand-off at the leading edge is slightly over-predicted but is acceptable. Away from the bow region, the experimental shock is located much closer to the body than that simulated. The small difference at the bow is most likely to be that the exact location of the jet head in the experiment is somewhat ambiguous due to the surrounding vapour and droplet cloud. Two other reasons for the difference are firstly, the computational results are for a steady state solution whereas the jet is growing. The shock is therefore a transient phenomenon, evolving as the jet geometry changes. The second is that

the interface between the liquid and the gas is not a solid wall. As the liquid jet is atomized, the core becomes increasingly porous so that some airflow diffuses into the quasi-porous medium. Ben-Dor et al. [27] suggest that the bow shock wave in front of porous materials quickly attenuates. Hence, the resultant shock will move towards the body. Away from the jet head, the agreement deteriorates. Incorporation of a cavity, that is, a sudden reduction in jet cross-section behind the jet head as suggested by Bloor [28] was examined as on Figure 15(b) but provided only marginal improvement. It is therefore believed that this simulation difference is due to the jet transience and porosity. It is noted that a similar comparison for a 2000 m/s jet gave very close agreement to experiment (Figure 16), probably because of a more coherent core and a slower attenuation.

Vapour and liquid jet solutions. While numerical evaluation of the shock structure for an equivalent solid body when compared to experiments with the liquid jet sheds some light on the nature of the processes, a simulation of fluid jets is a much more important step. The effect the shock has on the jet head and an understanding of the mixing of the liquid and air is essential for subsequent combustion studies of a fuel jet. This was undertaken with the use of the species transport equations in FLUENT. The mass concentrations in the mixing region used a species (O_2, N_2, H_2O) convection-diffusion equation. The method uses the FLUENT models for jet breakup and mixing that do not give atomisation details but indicate the local mass fraction of each species.
Previous work on subsonic jets has considered the instabilities in a jet, their effect upon the atomization process and the pressure distribution in the jet and has predicted droplet size and distribution. The most pertinent to the present study is the work of Bloor [28] who incorporated the numerical equations for supersonic flow into the computational solver, splitting the physical phenomena into a numerical domain constructed of layers, each being dependent on their respective boundary conditions. Resnyansky et al. [29] investigated the shock wave propagation in a one-dimensional, unsteady, two-phase flow. Their method does not predict atomization but generates a local mass fraction for the mixing layers that can describe mixing dependent phenomena.

In the current work, the ability of the numerical code to solve supersonic, multi-phase flows was studied with emerging jets as either vapour or liquid. This was initially undertaken as a steady state solution to illustrate core jet formation and mixing layer interactions. The governing equations in their unsteady form were then solved. While detailed comparison with the core jet from experiment was not possible, the transient numerical approach was tested by comparison against the jet shape and position over its life span from experiment. In the simulations, the assumptions are that:

- the jet is axi-symmetric.
- the liquid inlet boundary has a constant mass flow rate
- the liquid and gas are immiscible.
- the liquid is incompressible.
- the gas (air or vapour) is compressible, obeying the ideal gas law.
- the density ratio gives a species mass fraction concentration in the mixing layer.

Steady, supersonic jets. For these solutions, the jet initially at the simulated velocity (issuing at 600 m/s) is assumed to be in a fully developed state. It exists fully across the computational domain. Hence, the head of the jet is not considered and no shock waves are formed. At exit from the nozzle, it consists entirely of the either the water vapour or liquid (mass fraction = 1) as specified. This is the core jet. As the distance from the nozzle increases, the core reduces and the mixing layer increases. At a large distance along the jet axis, the core has become quite small. The simulation basically examines the aerodynamic processes in the shear layer that provide the breakup and mixing of the jet**.**

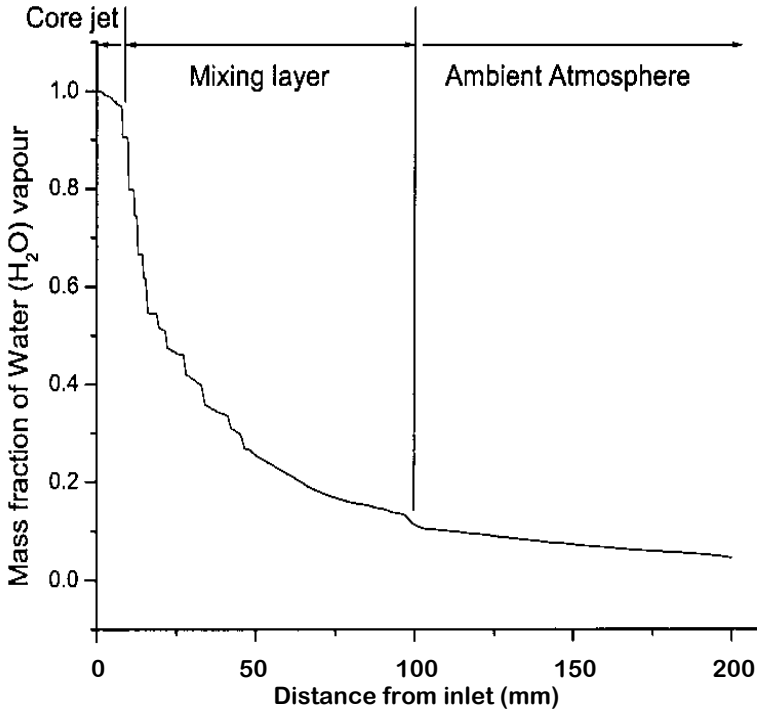

Figure 17. Vapour mass fraction profile for the steady vapour jet

The vapour jet. The vapour simulation assumes that the injected fluid is water vapour (H_2O) with density 0.55 kg/m^3. It could be envisaged that it is liquid water instantaneously expanded to atmospheric pressure, atomized and vaporized at the nozzle exit. The air consists of oxygen (O_2) and nitrogen (N_2) with a mass fraction of 0.23 and 0.77 respectively. In these calculations, the computational model uses the assumption that all species, including those in the mixing region are ideal gases. The solver computes for the three species, each having its own diffusion coefficient for predicting the interactive behaviour with other species. As all the species follow the ideal gas law, the solver is able to use a global density model.

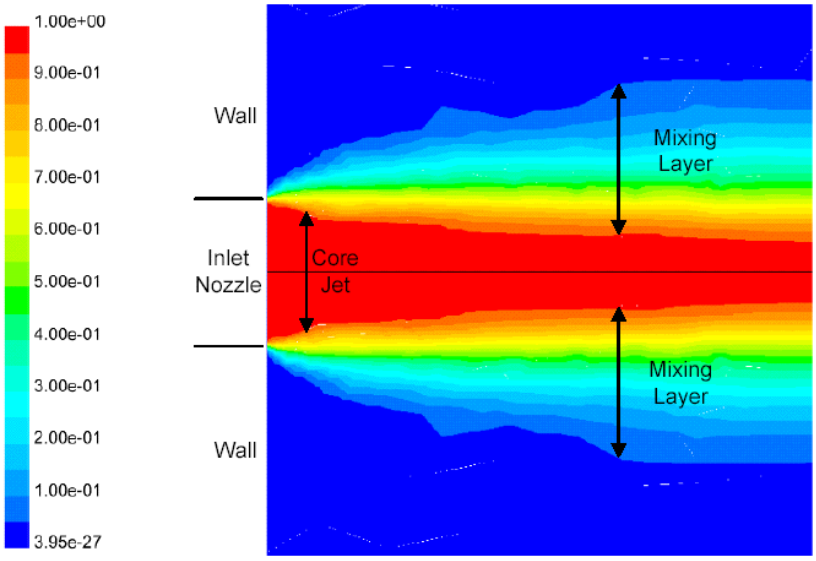

Figure 18. Core jet and mixing layer mass fractions for the steady vapour jet

The profile of a water vapour jet issuing from the nozzle at 600 m/s is shown in Figure 17. The trend in the mass fraction of vapour along the axi–symmetric boundary illustrates three regions in the formation of the jet as noted by other researchers. The mixing layer is arbitrarily defined as the region between a vapour mass fraction of 0.1 and 1. Using these definitions, the core jet, about 10 mm long, is the initial outflow of vapour into the atmosphere primarily consisting of the issuing fluid. A steep gradient then exists in the mixing layer where the vapour and air interact. This progressively becomes less steep as it approaches the ambient air atmosphere. The density ratio and the mixing law determine the properties in this region. The ambient atmosphere is the region barely affected by the issuing jet and has conditions that approach atmospheric.

Figure 18 illustrates the core and the distribution in the mixing layer. Immediately at the nozzle exit, the core jet has the same length scale as the nozzle diameter. As in Figure 17, the initially steep mixing gradient narrows the core sharply near the nozzle. Downstream, the rate of change in the core diameter reduces. As the core jet diameter decreases, the mixing layer profile increases. The jet is fully mixed when the core terminates. This is off the scale of the figure.

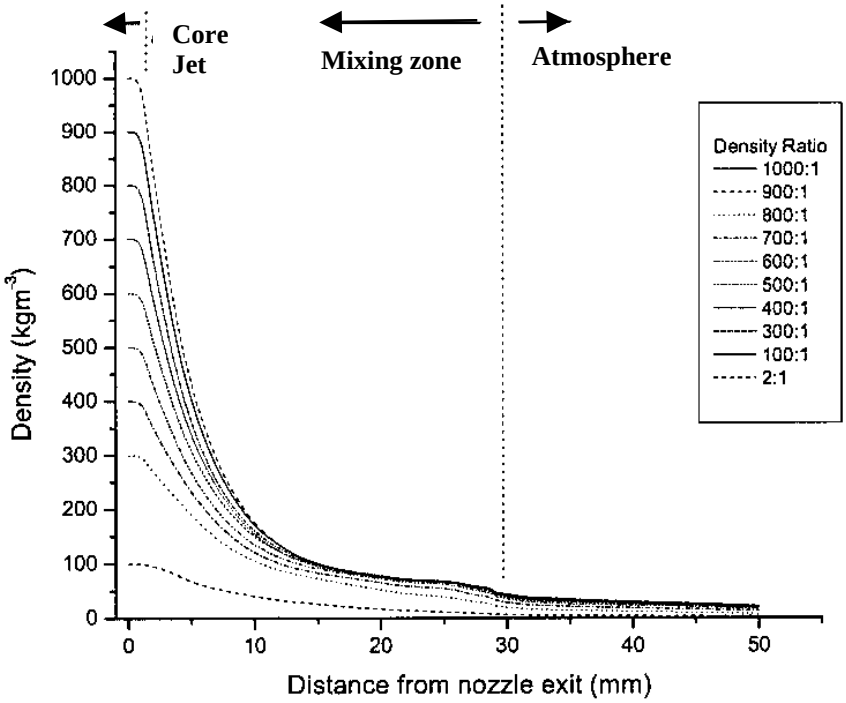

Figure 19. Steady liquid jet. Density variation for the jet through the mixing layer as a function of the initial density ratio chosen for the calculation. .

The liquid jet. With the liquid jet, the computation is more difficult because the governing relationships between the multi-species flows require the liquid to be set at constant density while the air is taken as an ideal gas. Because the density ratio of liquid to air is about 1000: 1, a further high gradient has to be resolved in the numerical scheme.

The default settings for FLUENT is that the density law for each species can only be set to a value that is either constant or determined from the ideal gas or quasi-ideal gas laws. Each species has to obey the same law. The code may be modified by the addition of compiled Used Defined Functions (UDF). This provides the ability to use an individual density law for each species. However, it adds considerably to the numerical stiffness and the additional computational time is extensive. The UDF assumptions made here are that the liquid has a constant density; the gas follows the ideal gas law density and the mixture fractions are determined from a volume-weighted law.

The inclusion of the UDF function means that the solver stability is decreased and a steady state solution cannot be easily achieved. Divergence occurs rapidly. To overcome this, a high node-density grid was found to be necessary. However, the computational time was very long. For the steady state case, this was reduced by use of a pre-solution adaptive technique In the pre-adaptive approach, a converged solution for a low density ratio (approximately 2) is obtained first. This is numerically stable. Its output data is then used to initialise a calculation for a small increase in the density ratio that again produces a stable solution, which in turn is used to initialise the next step. That is, by stepwise increasing the density ratio between the liquid jet and air from a low value, a stable solution is obtained for the high density gradient of liquid to air. While this iterative process is computationally expensive, it is less so than the high node-density mesh by itself.

For the 600 m/s liquid jet, a steady state solution was computed, the liquid density eventually being set to 998 kg/m^3 using the UDF function with the ideal gas relationship for the low density N_2-O_2 mixture. Results for initial liquid density ratios from 2 to 1000 are shown on Figure 19. As with the vapour jet, the core jet, mixing layer and atmosphere are clearly discernible. The intact core is only a few millimeters long while the mixing layer extends to 30 mm. A through-jet profile (Figure 20) also illustrates the mixing process.

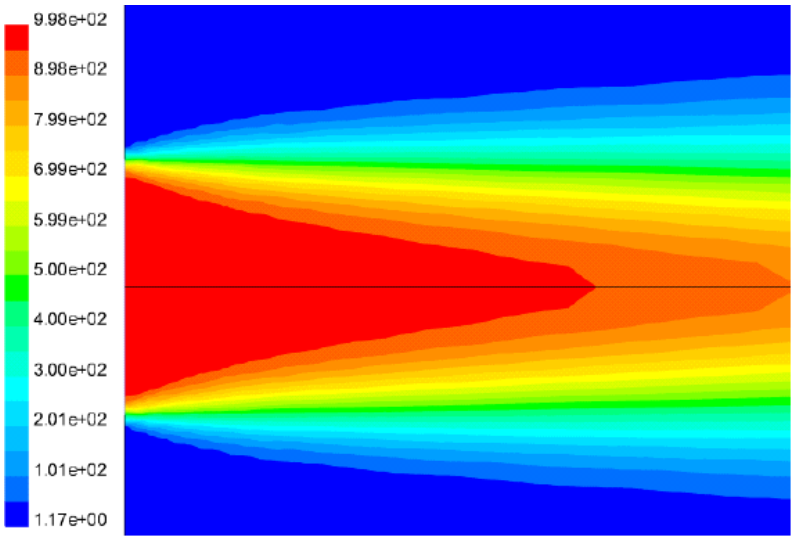

Figure 20. Core jet and mixing layer distribution for the steady liquid jet, showing mixture density (kg/m^3):

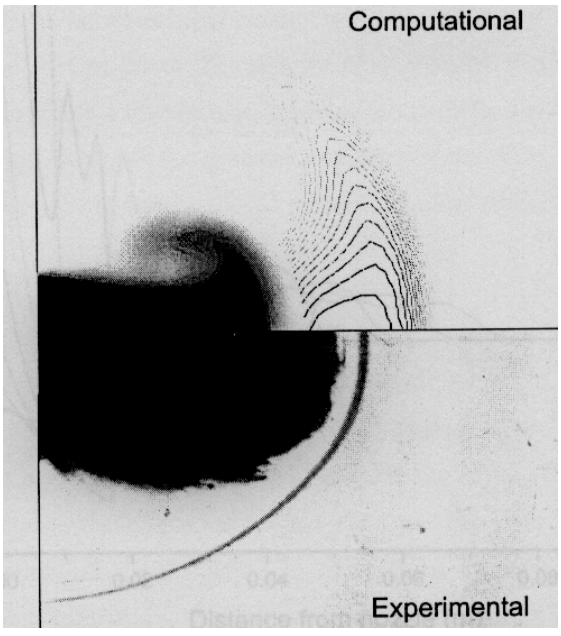

Figure 21. Simulation-experiment comparison for the shock wave from the unsteady vapour jet

Unsteady supersonic jets.

The vapour jet. In unsteady calculations, the jet efflux from the nozzle and the effect on the atmospheric air is integrated over time, the vapour jet calculations converging readily. A detached shock wave now appears at the leading edge of the jet as shown on Figure 21 although it is somewhat smeared. A higher node grid could resolve this more precisely at the expense of greater computational time. The fluid regime properties are calculated at each time step. The

unsteady equations track the path of the liquid jet head and hence predict its change of shape, intensification and attenuation. The shock will dissipate completely at time approaching infinity, this being the steady state solution. Figure 22 shows typical solutions for the vapour mass fraction.

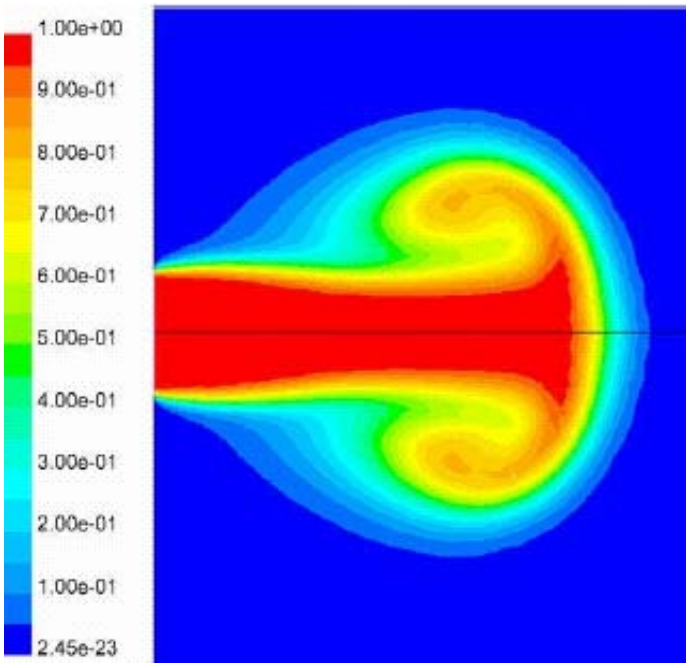

Figure 22. Mass fractions at 100 μs for the for the unsteady vapour jet

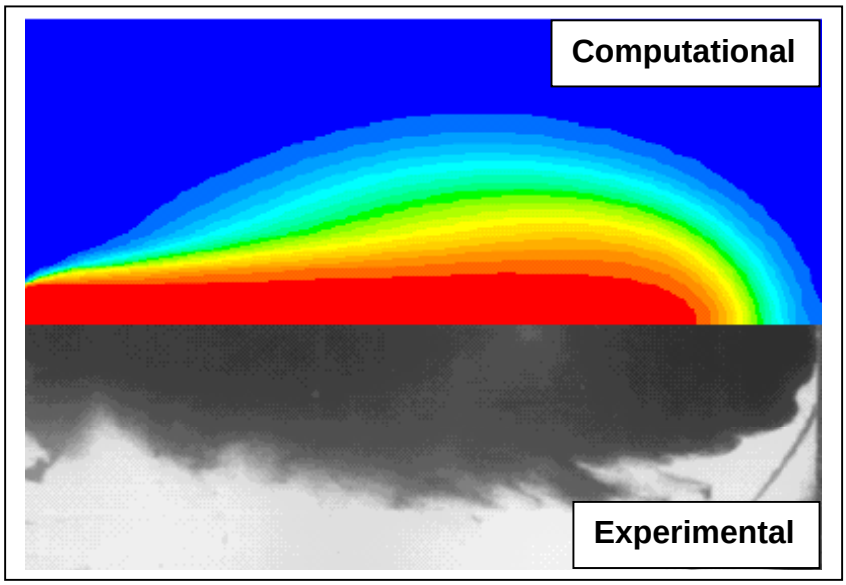

Figure 23. Comparison of simulated and experimental jet shapes for the unsteady liquid jet

The liquid jet. For the unsteady liquid jets, the high density gradients of the steady jets remain. However, it was not possible to implement the pre-adaptive technique and the high node-density mesh was utilized unaided. Computational time became very high, approximately 10 hours per time step and fewer cases could then be studied. The jet, on emerging from the nozzle, immediately accelerates the quiescent air ahead of it. The simulated jet shape is compared with experiment on Figure 23. Shapes are very similar with the simulation being a little wider further back from the jet head. This may be simply due to the experimental technique not picking up the very low liquid

fractions at the outer edge of the shear layer. The simulated surface is also smoother without the aerodynamically developed ligaments and this is due to deficiencies in the default models that were used from the code. The simulation shows the core jet with parallel sides and a radius approximately one-third of the outer radius. A typical radial mass fraction profile is shown on Figure 24.

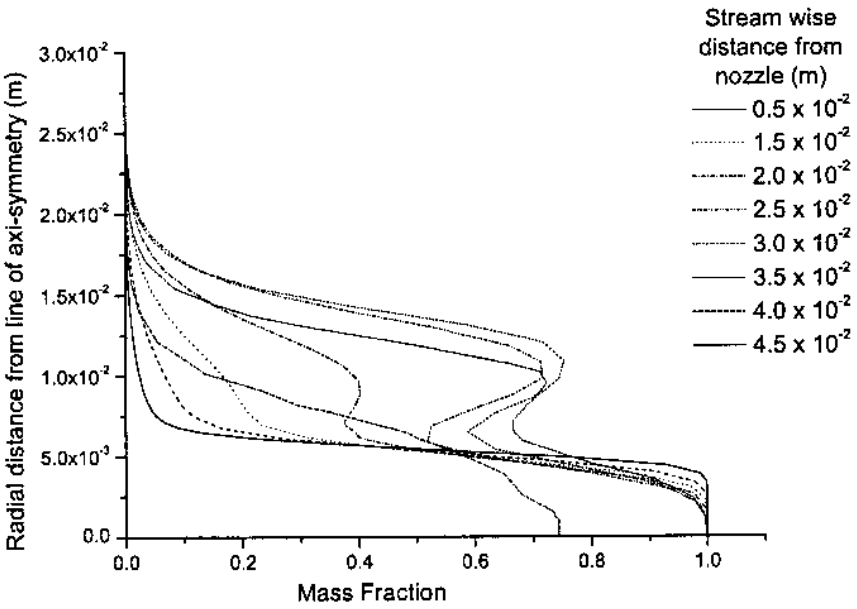

Figure 13. Unsteady liquid jet: Radial mass fractions at 120 μs

CONCLUSIONS

This paper has summarised work on pulsed, supersonic liquid fuel jets. These have been studied experimentally for low and high range supersonic Mach numbers and simulated for the low Mach numbers only. Both experiments and simulation are complex. The experiments have evaluated the velocities obtainable, the shock wave and jet structure in the external flow and the potential for autoignition of diesel type fuels. Nozzle shapes and materials have been evaluated and the jet attenuation and penetration studied. The latter show some similarity to the trends calculated from empirical formulas used for high subsonic diesel jets although the specific values need to be re-assessed. Several new phenomena have been found, these being, in particular a secondary and tertiary shock wave system.

The numerical studies have used a 1D analysis and the Autodyne code for assessment of the internal pressure rise due to the impact of the driving projectile. The 1D approach provides answers with values higher than experiment that fit a realistic coefficient of velocity of between 0.6 and 0.7. The Autodyne code gives values slightly lower than experiment in the later stages of the jet but is useful in that it also simulates the shock wave pressure rise through the nozzle walls.

For the external jet, the FLUENT code has been used. Its application has taken considerable development and has progressed through a solid body assessment of the bow shock waves for both low and high supersonic cases, steady vapour and liquid jets and unsteady vapour and liquid jets for the low supersonic case only at this stage. While some differences in the overall shock wave patterns and jet shape exist, particularly in regard to the former, the results are generally in reasonable agreement with experiment. This allows such things as the mixing layer to be evaluated

which is important for further incorporation into engine combustion codes. It must be emphasised that, at this stage, results are still preliminary and more development is required.

The value of increasing fuel injection pressures above current values for fuel jets in engines is still unclear. Some experiments indicate that there are further benefits on atomisation for pressures above about 250 MPa, others do not. However, in the 250 to 300 MPa range usually considered, the shock wave effects are either non-existent or negligible. A considerable increase in magnitude of the jet may be significant due to the formation of strong shock waves as shown here. The full effect of these waves remains unclear. While no autoignition was found in the current series of tests, fuel vaporisation was certainly enhanced. Thus, promotion of autoignition is likely and further tests, starting from known combustion conditions, (e.g. about 3 MPa and 500^{o}C ambient) should be considered. Increasing the jet velocity while working downwards in pressure and temperature would define the autoignition envelope for such high pressure jets.

On the fundamental side, good spray atomisation is essential. The single-hole, conical or smooth nozzles used in these experiments seemed to promote some additional atomisation although a good comparison with subsonic equivalents is needed. The sharp edge nozzle changed the spray pattern significantly, making it bushier. Nozzles with passageways approaching those of diesel injectors are under consideration with studies to maximise the cavitation within the nozzle. Further experiments with these in the low supersonic range are to be carried out.

Improved modelling of the jet development processes is essential. Much has been learnt from the current approach both of the flow within the nozzle sac from the 1D analysis and the Autodyne code. The same is true for the external flow modelled by the Fluent CFD code in relation to the shock structures and a preliminary assessment of the mixing. However, these approaches now need to be coupled so that the inflow boundary to the spray incorporates the unsteady velocity. A full atomisation model needs to be incorporated and the relative effects of aerodynamic shear, turbulence and cavitation evaluated. It may beneficial to develop a numerical scheme specific to this problem

The use of very high pressure jets as used in jet cutting may have limitations in engines due to the potential for damage, either to the nozzle, cylinder walls or piston. However, jets used for cutting purposes are coherent and the greater spray angle and finer atomisation of turbulent or cavitating nozzles should reduce this problem. The measured penetration distances, even with the 2000 m/s jets, are not unreasonable. Jets of around 600 to 1000 m/s should further minimise potential damage. The maximum injection pressures that can reasonably be used need to be explored. Jet velocity, engine size and air swirl need to be matched in any consideration of this type.

At present, further experiments are being carried out using more volatile fuels, these being butane, propane ethane and methane liquefied at low temperatures. These are all alternative fuels with low cetane numbers. Enhancing their ignitability would be beneficial.

Finally, an experimental and numerical study of supersonic fuel jets injected as a cross flow into a supersonic airstream needs to be undertaken. Very complex interactions will occur that may enhance scramjet combustion using liquid fuels. Modelling the shock wave interactions alone would provide a considerable and interesting task.

REFERENCES

1. Cummins, C.L., *Diesel's engine – Volume 1, From conception to 1918*, Carnot Press, Oregon, 1993

2. Field, J.E. and Lesser M.B., On the mechanics of high speed liquid jets, *Proc. Royal Soc. London. Series A*, Vol. 357, pp. 143-162, 1977.

3. Shi, H.H., Study of hypersonic liquid jet, *Ph.D. Thesis*, Tohoku University, Japan, 1994.

4. Shi, H.H. and Takayama, K., Generation of hypersonic liquid fuel jets accompanying self-combustion, *Shock Wave J.*, Vol. 9, pp.327-332, 1999.

5. Xu, S., Archer, R.D. and Milton, B.E., Injection of liquid hydrocarbon jets normal to supersonic airflows, *Proc. Int. Symp Shock Waves*, *ISSW22*, London, pp 1525-1530, 1999.

6. Jenkins D.C., Erosion of surfaces by liquid drops, *Nature*, Vol. 176, pp. 303-304, 1955.

7. Bowden F.P. and Brunton J.H., Damage to solids by liquid impact at supersonic speeds, *Nature*, Vol. 181, pp. 873-875, 1958.

8. Bowden F.P. and Brunton J.H., The deformation of solids by liquid impact at supersonic speeds, *Proc. Royal Soc. London, Series A*, vol. 263, pp. 433-450, 1961.

9. Huh, K.Y. and Gosman, A.D., A phenomenological model of diesel spray atomization, *Proc. Int. Conf. Multiphase Flows*, Tsukuba, Japan, 1991

10. Chaves, H., Knapp, M., Kubitzek, A., Obermeier, F., and Schnieder, T., Experimental study of cavitation in the nozzle hole of diesel injectors using transparent nozzles, *SAE paper 950290*, 1995.

11. Soteriou, C.C.E., Andrews, R.J. and Smith, M., Direct injection diesel sprays and their effect of cavitation and hydraulic flip on atomization, *SAE paper 950080*, 1995.

12. Reitz R.D. and Bracco F.V., Mechanism of atomization of a liquid jet. *Phys Fluids*, Vol. 2(5): pp. 1730-1742, 1982.

13. Hiroyasu, H., Fundamental spray combustion mechanism and structures of fuel sprays in diesel engines, in *Mechanics and Combustion of Droplets and Sprays*, Ed. Chui, H.H. and Chigier, N., Begell House, NY, 1995.

14. Nishida, K., Ochiai, H., Arai, M. and Hiroyasu, H., Characterization of diesel fuel spray by ultrahigh-pressure injection, *Trans. Japan Soc. Mech. Eng.*, Part B, Vol. 63(605), pp. 344-349, (in Japanese), 1997.

15. Choi, I.S. and Milton, B.E, A Dual-Fuel Combustion Model for Pre-Mixed Natural Gas with Distillate Ignition in a Quiescent Bomb, *Numerical Heat Transfer, Part A*:, Vol. 31, No. 7, pp. 725- 743, 1997.

16. Mbarawa, M., Milton, B.E. and Casey, R.T., Experiments and Modelling of Natural Gas Combustion Ignited by a Pilot Diesel Fuel Spray, *Int. J. Thermal Sciences*. Vol 40, pp 927- 936, 2001.

17. Miao, H. and Milton, B.E. Modelling of the gas/diesel dual-fuel combustion process for conditions applicable to engines, *Numerical Heat Transfer*, Part A, Vol. 41, pp 725 –739, 2002.

18. Arcoumanis, C. and Gavaises, M., Linking Nozzle Flow with Spray Characteristics in a Diesel Fuel Injection System, *J. Atomization and Sprays*, Vol. 8, pp. 307-347, 1998.

19. O'Keefe J.D., Wrinkle W.W., and Scully C.N., Supersonic liquid jets, *Nature*, Vol. 213, pp. 23-25, 1967.

20. Ryhming I.L., Analysis of unsteady incompressible jet nozzle flow, *J. Applied Maths. and Phys. (ZAMP)*, Vol. 24, pp. 149-164, 1973.

21. Glenn L.A., The mechanics of the impulse water cannon, *Computers & Fluids*, Vol. 3, pp. 197-215, 1975.

22. Lesser M., Thirty years of liquid impact research, *Wear*, vol. 186, pp. 28-34, 1995.

23. Pianthong K., Milton B.E. and Behnia M., Generation and Shock Wave Characteristics of Unsteady Pulsed Supersonic Liquid Jets, *J Atomization and Spray*, in press, no. 5-6, 2003

24. Pianthong K., Zakrzewski, S., Milton B.E. and Behnia, M., Supersonic Liquid Jets: Their Generation and Shock Wave Characteristics, *Shock Wave J*., Vol. 11, No. 6, pp 457-466, 2002

25. Pianthong, K., Milton, B.E. and Behnia, M., Fundamentals of Supersonic Diesel Fuel Jets for use in Diesel Engines, *12th Int. Pacific Conf. on Automotive Eng*., Thailand, Paper D08, 2003.

26. Zakrzewski, S., Behnia, M., Milton, B.E., A Blunt Body Analogy for Bow Shock Characteristics in Front of a Supersonic Liquid Jet, *Proc. 2nd Int. Conf. on Comp. Fluid Dynamics*, ICCFD2, Sydney, July, 2002

27. Ben-Dor, G., Britian A., Elperin, T., Igra, O. and Jaing J P, Experimental Investigations of the Interaction between Weak Shock Waves and Granular Layer, *Expt. in Fluids*, Vol. 2, No. 2, pp. 432-443, 1997.

28. Bloor, M.I.G., Hypersonic liquid jets, *J. Fluid Mech*. Vol. 84, No. 2, pp. 375-384, 1978

29. Resnyansky, A.D., Milton, B.E. and Romensky, E.I.. A Two-Phase Shock-Wave Model of Hypervelocity Liquid Jet Injection into Air. *JSME Cent. Grand Cong., Int. Conf. on Fluid Eng.*. Tokyo, 1997.

Acknowledgements: The author would like to acknowledge the major contributions of Dr. K. Pianthong, Dr. S Zakrzewski. Professor M. Behnia, Professor K. Takayama and Professor T. Saito on work directly related to supersonic jets, Professor S. Xu and Professor R.D. Archer for their work on subsonic injection into supersonic airstreams and Dr. I. Choi, Dr. M. Mbarawa and Dr. H Miao for their development of diesel jet and spray models.